Results of the First Defocus Particle Tracking Challenge

M.Rossi[1,*], S. Sachs[1,2,3,*], C. Cierpka[2,3]

1: Department of Industrial Engineering (DIN), University of Bologna, via Montaspro 97, 47121 Forlì, Italy
2: Institute of Thermodynamics and Fluid Mechanics, Technische Universtität Ilmenau, Werner-Heisenberg-Weg 1, 98693 Ilmenau, Germany
3: Institute of Micro- and Nanotechnologies (IMN) MacroNano, Technische Universtität Ilmenau, Gustav-Kirchhoffstraße 7, 98693 Ilmenau, Germany
*Corresponding author: massimiliano.rossi13@unibo.it

Keywords: defocusing, microfluidics, particle tracking velocimetry, thermometry.

ABSTRACT

This work presents the results of the First Defocus Particle Tracking (DPT) Challenge. The Challenge was structured with experimental and synthetic datasets. The experimental datasets consisted of a physical microfluidic device, the Chip-in-a-Box (ChiB), directly shipped to the interested participants. The synthetic datasets, referred to as the Multi-Flavour Datasets (MFDs), consisted of images generated with a ray-tracing approach capable of generating different types of defocusing images with a unified methodology. Seven international research teams submitted results in at least one case of the Challenge. A great variety of established defocus-based approaches (or flavors) was reflected by the contributing teams, spanning from three-pinhole techniques and shadowgraphy to astigmatism particle tracking. Five teams submitted results for the experimental test cases and applied a DPT method with their favorite flavor in one microfluidic experiment in the ChiB. By optimizing the experimental conditions, reliable particle tracking with a spatial resolution of up to 2.7×10^{-2} velocity vectors per μm^3 was achieved in two demanding benchmark experiments. Five teams submitted results for synthetic MFDs showing overall excellent results, with median errors down to 0.017 pixel for the in-plane coordinate and 0.17 pixel (0.07 % of the full depth size) for the depth coordinate up to a particle image density of 0.0016 particles-per-pixel (ppp). The results demonstrate that DPT evolved as a versatile and precise measurement technique, encompassing a broad spectrum of methodological flavors.

1. Introduction

The organization of periodic Challenges is a well-established practice in the PIV community, and it has substantially contributed to the progress of various techniques [1, 2]. This Challenge, first of its kind, focuses on the assessment of DPT methods, which are single-camera, three-dimensional (3D) particle tracking techniques, where the depth (out-of-plane) coordinate is derived from the degree of defocusing of the particle images. DPT methods have been predominantly used for 3D particle tracking in microfluidic applications [3], but they have recently attracted interest in other fields such as sprays [4] and wall shear stress measurements [5].

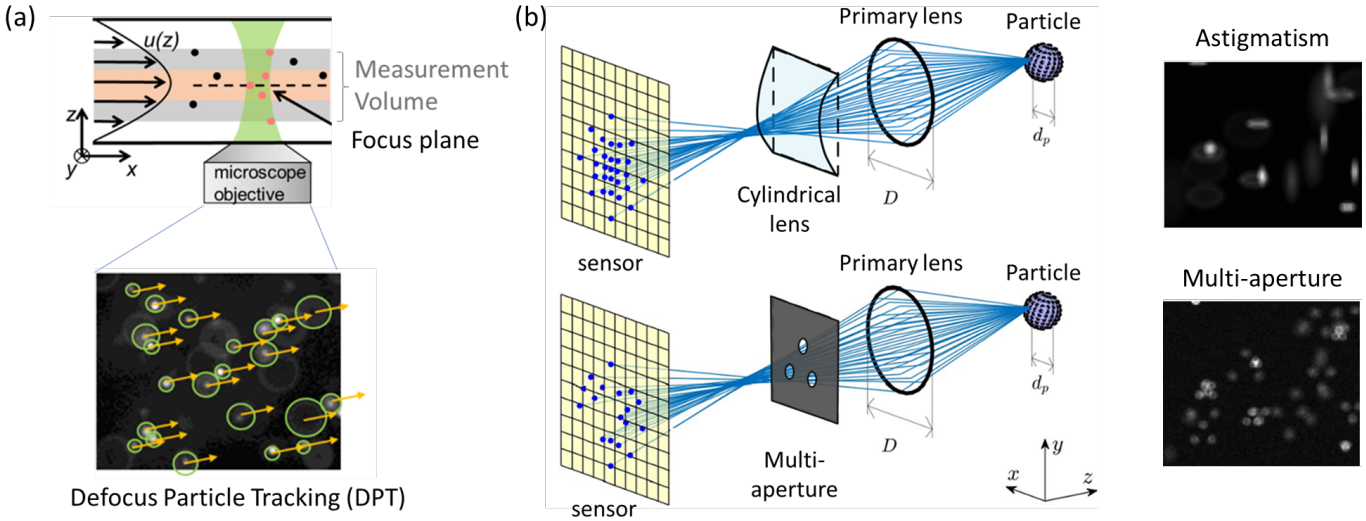


Figure 1. Fundamentals of DPT methods: (a) The degree of defocusing of particle images is used to determine the out-of-plane coordinate. (b) Different approaches can be used to encode more efficiently the defocusing information, such as a cylindrical lens or a pinhole mask.

One characteristic of DPT methods is that while the fundamental information about the depth position is encoded in the degree of defocusing of the particle images, different approaches have been developed to read out this information more efficiently (Fig.1). Notable examples are the use of multi-aperture masks (here referred to as pinhole) behind the lens [6] or a cylindrical lens to induce an astigmatic aberration [7]. Other DPT techniques employ a shadograph approach for forming the particle image [8], which also impacts the final result.

Most works in the literature investigate and compare the uncertainty of one specific approach (here referred to as "flavor"), making it quite difficult to assess the strengths and limitations of the different approaches on a fair and quantitative basis. On the other hand, designing test cases that can account for the different flavors and provide comparable results is not straightforward. To solve this problem, the current Challenge offers two different families of test cases:

1. An experimental test case, referred to as Chip-in-the-Box (ChiB), which is a physical microfluidic device directly shipped to the participants. The ChiB consists of a microchannel with channel side walls made of dry film resist (DFR) and a channel ceiling and bottom made of glass to provide optical access for illumination and image recording. The devices can be fabricated with high repeatability [9], thus providing all the participants with an identical battlefield. The participants can use any DPT technique of their choice to measure the flow field in two specific sections of the device. The only limitations are that the technique must belong to the DPT family (single-camera approach based on defocusing) and that the experiments must be carried out according to a specified set of operating conditions.

2. A set of synthetic datasets, referred to as the Multi-flavor Datasets (MFDs), which are gen-

erated using a synthetic image generator (SIG) based on ray tracing [10]. The ray tracing approach allows us to replicate the datasets with the same basic characteristics (position of the tracer particles, number of images, characteristics of the primary optics), for the different flavors, as schematized in Fig.1b. A total of three MFDs has been prepared, each assessing different aspects of DPT methods.

The Challenge and the main characteristics of the test cases (ChiB and MFDs) were presented in June 2025 at the 16th International Symposium on Particle Image Velocimetry in Tokyo [11]. The Challenge officially opened on November 25, 2025, with a dedicated website (https://www.tu-ilmenau.de/defocus) for registration and requests for test cases. Each team was allowed to participate in a single family of test cases (ChiB or MFDs) or in both. The final deadline for submitting results was set for the end of May 2026. From a group of 10 research groups registered for the Challenge, a total of 7 teams submitted results for one family of test cases or both, summarized in Table 1. The present conference contribution provides an overview of the submitted results from the different teams and the major outcomes of this initiative. A follow-up journal publication with a detailed presentation and comparison of quantitative metrics is planned after the conference.

Table 1. Research groups participating in the challenge

	ChiB	MFD
BiRe Track	C	-
FIL	A	1
GW	A, B	1
LaVision	-	1, 2, 3
Madeira	-	1, 3
MorePath	A	1, 2, 3
Taiwan Tech	A	-

2. Preparation of the test cases

2.1. Chip-in-the-Box (ChiB)

In Fig. 2a and b, the design and a photograph of the ChiB are depicted from a top view, respectively. Along the microchannel with a cross-section of $200 \times 165\,\mu\mathrm{m}^2$, measurements were taken at two specific test sections at different operational conditions. On the one hand, a backward facing step with a step height of $110\,\mu\mathrm{m}$ is located in test section 1. By using different DPT techniques, all three spatial coordinates and velocity components (3D3C) were measured at a flow rate of either

$10\,\mu L\,min^{-1}$ (referred to as test case A) or $300\,\mu L\,min^{-1}$ (referred to as test case B) by the participants. The expected velocity fields differ significantly as depicted by the velocity component w in the xz-plane along the centerline of the microchannel in Fig. 2c and d using numerical results, respectively. While a pronounced out-of-plane velocity is present in both cases, the formation of a recirculation region is evident only in the high flow rate case.

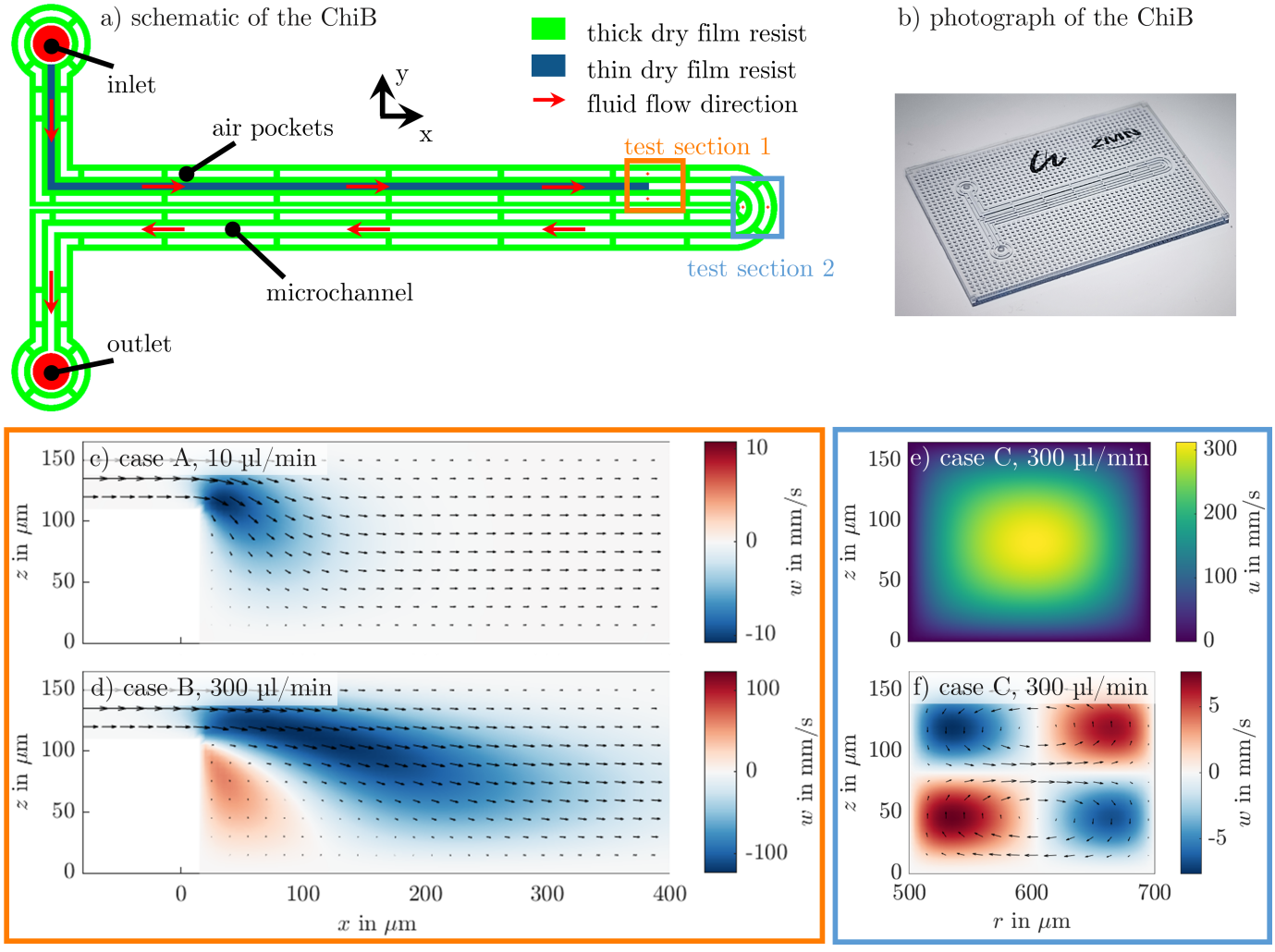


Figure 2. (a) Schematic of the ChiB, showing the two test sections where the experiments were conducted. (b) Photograph of the fabricated ChiB. In (c) and (d), the velocity component w derived numerically for test section 1 as reference for the test cases A and B are depicted, respectively. In (e) and (f), the velocity components u and w for test case C in test section 2 are shown, respectively.

On the other hand, a Dean flow is expected to develop in the curved microchannel at test section 2 by applying a flow rate of $300\,\mu L\,min^{-1}$ (referred to as test case C). In Fig. 2e and f, the numerically derived velocity components u in main flow direction and w in depth direction are shown in the channel cross-section at the apex of the curve. The stationary axial-symmetric flow has a complex pattern with velocity components in the channel cross-section that are significantly lower than in

main flow direction, providing a demanding test case for DPT techniques.

In all experimental cases, the measurement uncertainty and deviation from a reference flow field obtained from numerical simulations will be evaluated based on Lagrangian and Eulerian data measured in the ChiB. The illumination, particle size, and seeding concentration can be set freely by the participants to achieve the optimal result. The choice of the interpolation procedure for the reconstruction of the Eulerian data from the Lagrangian trajectories is also left to the participants' discretion.

2.2. Multi-flavor Datasets (MFDs)

The MFDs are a first attempt to provide a comparative analysis of different DPT methods using a unified system for generating synthetic images. The underlying concept is that all DPT methods rely on the same principle: Tracer particles are observed with an optical system with a small depth of field, and their depth position is encoded in the defocusing pattern of the corresponding particle images. Using a synthetic image generator (SIG) based on ray tracing [10], it is possible to start from a unique main objective lens and generate different synthetic defocus particle images by

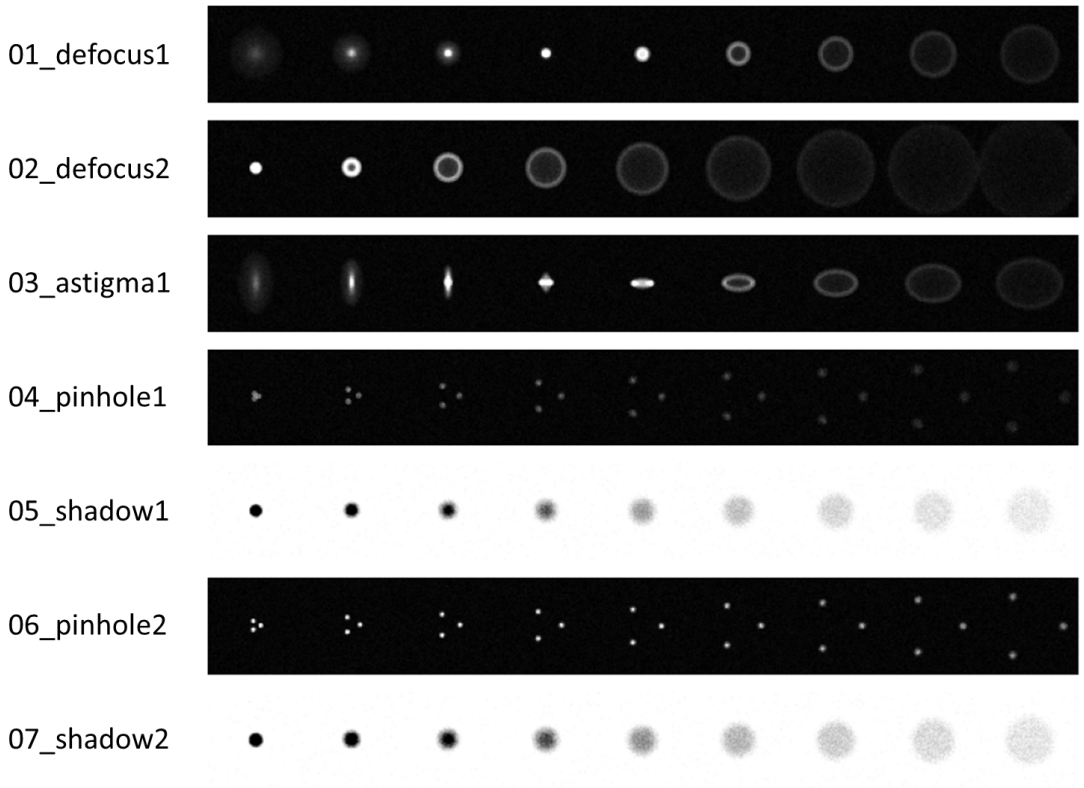


Figure 3. Defocused particle images across the full measurement depth for the seven flavors prepared for the Challenge. For every flavor, a virtual objective with a magnification of 10× and a numerical aperture (NA) of 0.15 was used. The gain was adjusted to reach approximately an average SNR similar for each case.

introducing different virtual optical elements along the optical path.

All the MFDs were generated using a virtual objective with a magnification of 10× and a numerical aperture (NA) of 0.15, coupled with a virtual sensor with a resolution of 1024 × 768 pixels, pixel size of 6.45 μm and a dynamic range of 12 bit. A total of 7 different settings, referred to as flavors, were generated for this challenge, corresponding to four families of DPT approaches: simple defocusing, astigmatism, three-pinhole, and shadowgraphy, as shown in Fig. 3. The measurement depth was fixed to 240 pixels (px) for all cases. It should be noted that for consistency with the uncertainty analysis, all dimensions, including the depth direction (Z) were given in pixels. For the depth direction, 240 px corresponded to a measurement depth of 154.8 μm.

Although this approach provides common ground, it is still quite difficult to guarantee a completely fair comparison, as many parameters remain in play. As an example, the three-pinhole method requires a much larger input intensity with respect to the astigmatic method [3], but the area occupied by the three-dotted particle images is much smaller than the corresponding area of an astigmatic particle image, giving an advantage in high-density flow. Another difference is given by the signal-to-noise ratio (SNR) profile across the depth for shadowgraphy images, which required larger particles to be compatible with fluorescent (brightfield) particles. The general choice for this Challenge was to maintain an average SNR similar for all flavors. This will inevitably affect the final results, and should be kept in mind when comparing the performance between different flavors. Three datasets were proposed for this challenge:

MFD1 The objective of MFD1 is to evaluate how the DPT methods deal with increasing particle image density, following the standard approach used earlier [12]. Six datasets were provided, starting with no overlapping particle images (ppp = 0) up to ppp = 0.0016. Upon request of one team, three optional cases were added for the flavor "06-pinhole2" with ppp = 0.02, 0.03, 0.1.

MFD2 The objective of MFD2 is to evaluate the sensitivity of DPT methods to non-monodispersed particle images. Images were generated with non-monodispersed tracer particles, with diameters randomly distributed with a standard deviation of 30% of the mean value.

MFD3 In the MFD3 a real case of a complex 3D flow was simulated. The flow (not disclosed before the closing of the Challenge) was a synthetic flow mimicking the flow structures inside an evaporating droplet with the coexistence of a capillary bulk flow and a thermally-induced Marangoni flow at the surface [13]. Part of the measurement volume was outside of the droplet surface and, therefore, without seeding particles. The requested measurement in this case were the Lagrangian particle trajectories and, optionally, an Eulerian reconstruction of the flow field using interpolation techniques.

For each dataset, calibration data were provided for 81 planes, equally spaced across the measurement depth.

3. Results

3.1. ChiB

In total, five groups participated in the three experimental cases A, B and C as listed in table 2, arranged by their group names. While four groups derived experimental results on the fluid flow across a backward facing step with a flow rate of $10\,\mu\mathrm{L\,min^{-1}}$ (case A), only one group contributed to each of the high flow rate cases at the step (case B) and curved channel section (case C). A great variety of experimental techniques was reflected by the participants, applying segmentation and tracking anything-based robust astigmatism particle tracking velocimetry (STAR-APTV [14], FIL), color-coded pinhole micro PTV (color-coded µPTV [15], Taiwan Tech), shadowgraphy [16, 17] (MorePath), micro-plenoptic [18] (GW), and double-refractive PTV (DRPTV [19], BiRe Track). Moreover, the experimental parameters were set quite differently among the groups. In particular, the size of the tracer particles used ranges from $1.7\,\mu\mathrm{m}$ up to $5.03\,\mu\mathrm{m}$, while all groups decided to use fluorescently labeled polystyrene particles. The particles were illuminated either by an LED or a laser with exposure times equal or below $1\,\mathrm{ms}$. Notably, the shortest illumination time was used by the group 'BiRe Track' at $10\,\mu\mathrm{s}$ to measure the Dean flow at a flow rate of $300\,\mu\mathrm{L\,min^{-1}}$, successfully preventing motion blur effects. Conversely, particle image streaks were successfully utilized by the group 'Taiwan Tech', which employed color-coded µPTV and an exposure time of $10\,\mathrm{ms}$. In this challenge, all freedom to choose the amount of acquired images and measurement positions across the depth direction was given to the participant. In turn, these quantitative scales were greatly used to enhance the experimental results. In particular, while only 100 images were taken by the group 'FIL' using the deep learning enhanced STAR-APTV, up to 29995 images

Table 2. Parameters used by the participants in the experimental test cases.

group name	BiRe Track	FIL	GW	MorePath	Taiwan Tech
technique	DRPTV	STAR-APTV	micro-plenoptic	shadowgraphy	color-coded µPTV
test cases	C	A	A/B	A	A
particles					
material	polystyrene	polystyrene	polystyrene	polystyrene	polystyrene
size	2.47 µm	5.03 µm	1.7 µm-2.2 µm	5 µm	1.54 µm
seeding	$17.8\,\mathrm{mg\,L^{-1}}$	0.306 (area fraction)	$13\,\mathrm{mg\,L^{-1}}$	0.001 ppp	1 ppm
illumination	Nd:YAG Laser	Nd:YAG Laser	Green LED	Blue LED	RGB LED
acquisition					
exposure time	10 µs	1 ms	100 µs	171 µs	10 ms
inter-frame time	400 µs	1 ms	769 µs	250 µs	22.2 ms
no. of images	18000 (DF)	100	26000	4000	29995
no. of z-planes	12	1	1	1	5
vectors	99254	807	186195	317638	6599
vectors per µm^3	2.7×10^{-2}	5.8×10^{-5}	1.3×10^{-2}	2.3×10^{-2}	4.8×10^{-3}
vectors per image	5.51	8.07	7.16	79.41	0.22

were recorded by 'Taiwan Tech'. Also, while most of the groups only used a single measurement position along the z-direction, the group 'BiRe Track' recorded double-frame images in 12 depth positions. The most efficient use of the recorded images was identified for 'MorePath', acquiring an average of 79.41 velocity vectors per image. 'MorePath' also achieved the second highest spatial resolution, surpassed only by 'BiRe Track' at 2.7×10^{-2} vectors per $\mu\mathrm{m}^3$.

In Fig. 4, typical raw images recorded by the participants are depicted. The variety in the visual appearance of the recorded images greatly reflects the versatility in resolving the depth position of the particles encoded in the images acquired by a single camera. In particular, raw images taken by 'FIL' and 'BiRe Track' strongly show astigmatic distortions of the particle images, either introduced by a cylindrical lens or a birefringent substrate in the optical path to the camera. Hence, the depth position of the particles is encoded in the shape of the particle images or, in case of DRPTV, the difference between the squared particle image diameters of ordinary and extraordinary particle images. In contrast, the distance between the particle images that form triplets in the three-pinhole method can be related to the z-position of the particle. Color-coding the triplets further facilitates the matching of the particle images, as demonstrated by 'Taiwan Tech'. In the shadowgraphic approach of 'MorePath', an AI-based calibration model was used to map the particle images to their corresponding depth position. Combining the high contrast in the raw images with the advanced YOLO-11 artificial neural network architecture for object detection clearly paid off, resulting in the highest number of detected velocity vectors per image. In an alternative approach, the group 'GW' employed a plenoptic camera in which a microlens array encodes angular information, allowing

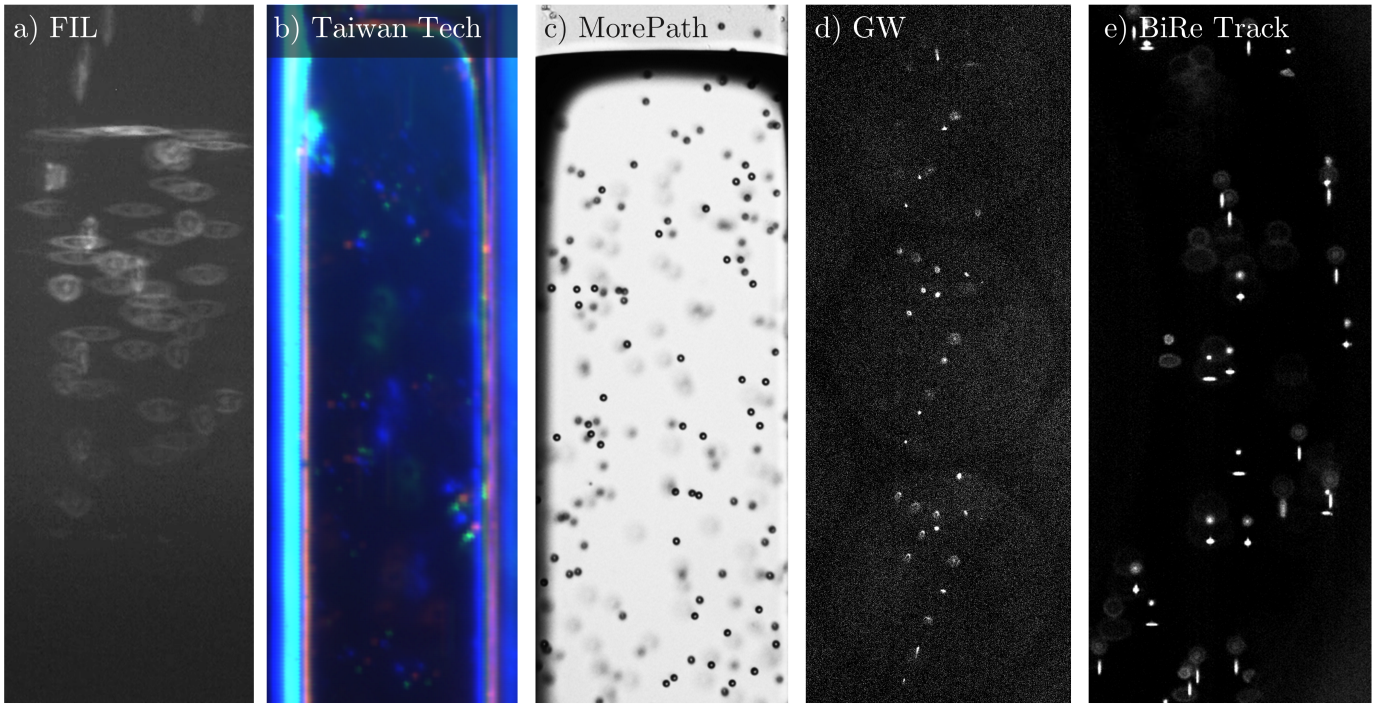


Figure 4. Raw images experimentally acquired by the participants in different sections of the ChiB.

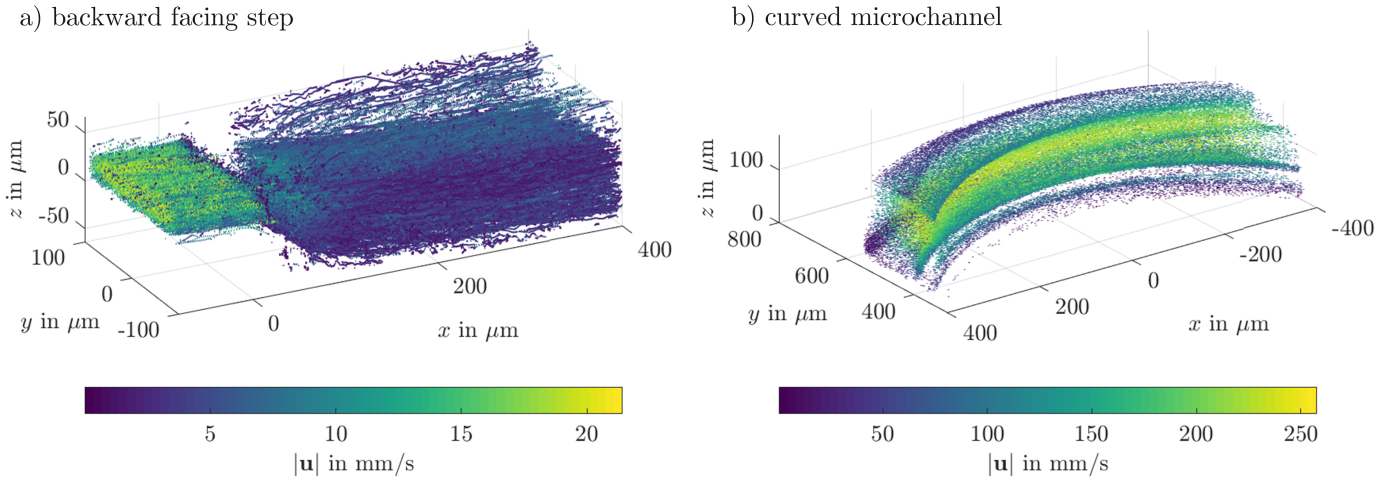


Figure 5. Three-dimensional Lagrangian velocity fields recorded by 'MorePath' at the backward facing step (a) and by 'BiRe Track' at the curved section of the microchannel (b).

to reconstruct the depth coordinates of the particles from multiple perspective views using only a single camera.

The measured Lagrangian velocity data at the backward facing step (case A) is exemplified by the results from 'MorePath' in Fig. 5a. Based on the color-coded absolute velocity in the microchannel, a reliable detection of both fast particles above the step and rather slow particles further downstream is demonstrated. As part of the light is blocked by the layer of dry film resist forming the step, this result confirms the robust application of AI-based approaches for particle detection in DPT. However, the number of detected particles dropped at the edge of the step due to shadowing effects as evident in the raw images depicted in Fig. 4c. Furthermore, the Lagrangian velocity data measured by 'BiRe Track' at the curved section of the microchannel is depicted in Fig. 5b. In accordance with the numerical simulation, a velocity exceeding $250\,\mathrm{mm\,s^{-1}}$ was confirmed experimentally. Compared to the high fluid velocity in main flow direction, the lateral velocity components in the channel cross-section were found to be approximately 25 times lower. The large difference in the magnitude of the velocity components puts significant challenges on balancing the experimental parameter of the measurement. In particular, the inter-frame time needs to be set sufficiently large to resolve the secondary flow components, while allowing for a robust particle matching without underestimating the main flow velocity. In this demanding setup, the reliable application of single camera defocus techniques was successfully demonstrated by 'BiRe Track' in excellent coherence with numerical simulations. At the conference, the Lagrangian and Eulerian velocity fields derived by the participating groups will be analyzed and compared to numerical simulations in greater detail.

Table 3. Summary of the results submitted by the participant for the MFDs.

group name	FIL	GW	LaVision	Madeira	MorePath
technique	CNN	CNN	IPR+STB	CNN + FFT	CNN
test cases	1	1	1,2,3	1,3	1,2,3
flavor	03	01, 02, 03, 04, 05, 06	06	01, 02, 03, 05, 07	05

3.2. MFDs

In general, all results submitted for the MFD case achieved very good accuracy and recall, outperforming earlier results in the literature [12]. All the teams submitted results for MFD1, two teams for MFD2, and three teams for MFD3. The summary of the submitted results are presented in Table 3. For all cases, the error was provided in terms of median absolute error (measured value - true value). To match true data with measured data, a nearest neighbour tracking algorithm was used. Matched particles with a distance larger than 15 px in the XY direction and 30 px in the Z direction were considered outliers. This conference contribution presents an overview of the main findings. In particular, MFD2 and MFD3 were covered only by a few groups and will be discussed only briefly here. A more comprehensive analysis, including a detailed uncertainty assessment and a thorough description of the methodologies employed, will be presented in a forthcoming journal publication.

Interestingly, four of the five teams used processing method based on convolutional neural network (CNN). The team 'FIL' used the same STAR-APTV approach [14] as in the experimental case, a deep-learning-assisted framework with additional post-processing and filtering strategies. They provide results for MFD1 with the '03-astigma1' flavor. The team 'GW' used a convolutional U-Net for simultaneous detection and localization of the particle images combining different techniques used in particle tracking [20] and single molecule localization [21]. They provided results for MFD1 for all flavors except for the last one. They trained a specific network for each flavor. The team 'LaVision' is the only one that did not use a CCN-based approach. The data is processed within the framework of Iterative Particle Reconstruction (IPR) [22, 23] and Shake-the-Box (STB) [24, 25] with few modifications necessary to adapt it to single-image multi-aperture data. They processed data with the flavor '06-pinhole2' and provided results for all MFDs. The team 'Madeira' used a hybrid approach: the in-plane position was determined using a generalized YOLO-based approach optimized for defocused particle images of arbitrary shapes [26] and the depth position was determined using a conventional approach based on cross-correlation (FFT) [12]. They processed data for all flavors except for the three-pinhole cases (04 and 06) and provided results for MFD1 and 3. The team 'MorePath' used a CNN-based approach based on YOLO for the in-plane localization and a ResNet for the out-of-plane determination [16, 17]. Their analysis was focused on the '05-shadow1' dataset and they provided results for all MFDs.

MFD1

All teams took part to the MFD1 case, so it is the most representative for this Challenge. As mentioned already, the results from all teams were very good and superior, even at the larger particle

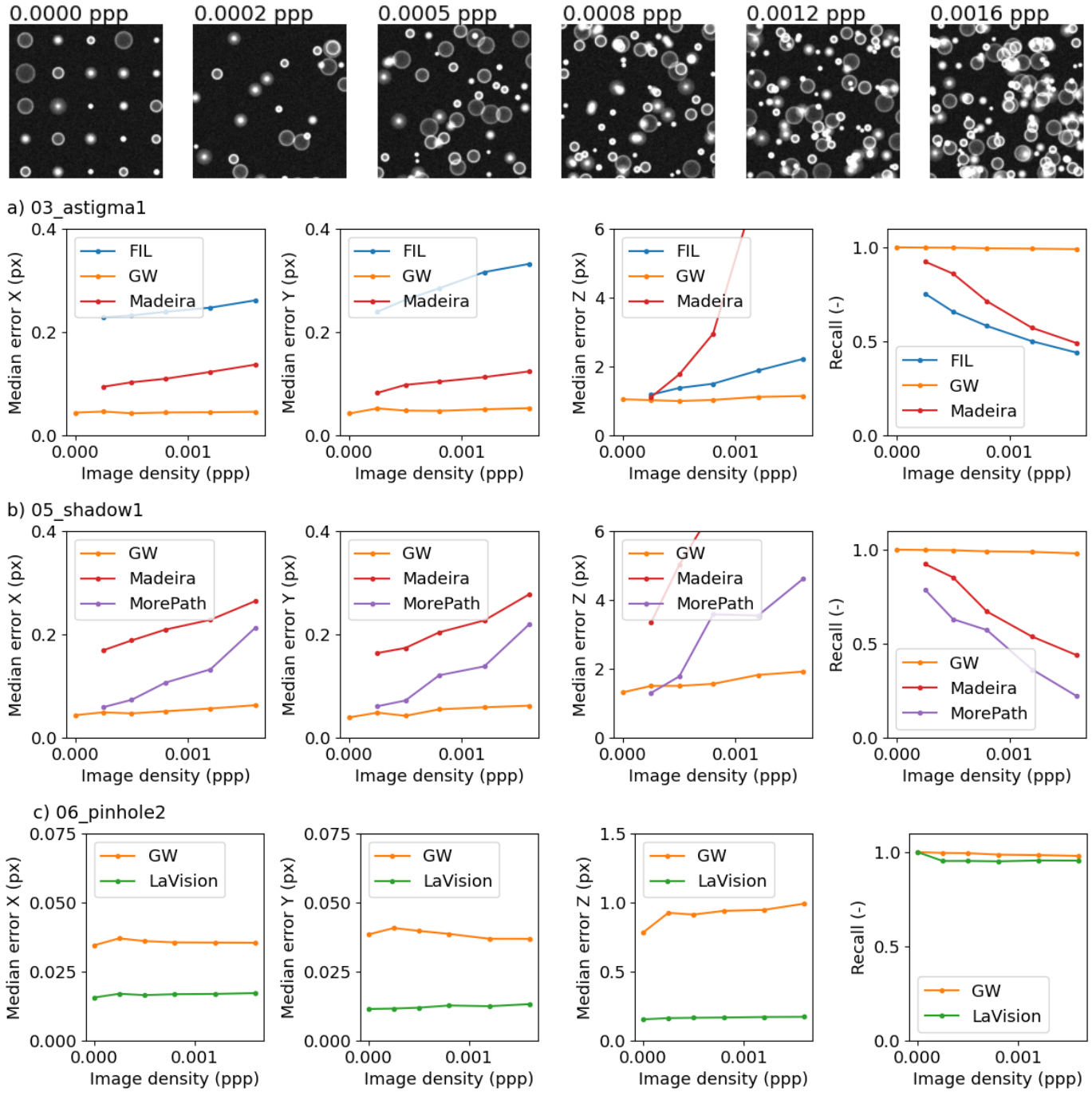


Figure 6. Median error in the position determination (X,Y, and Z) and recall versus image density for flavors (a) 03-astigma1, (b) 05-shadow1, and (c) 06-pinhole2. In the top line, an example of images from the flavor '01-pinhole1' are presented for increasing image density.

image density, to what was presented previously. For the low seeded cases, the in-plane errors were in general below 0.1 px and the depth errors below 2 px, which is below 1% error on the full depth length, the typical limit for conventional methods. For consistency, pixel units (px) were also used for the depth measurement. For larger particle image densities, the error is, in general, increasing as expected due to the effect of overlapping particles. Remarkably, the teams 'GW' and 'LaVision' showed that their code is very robust against overlapping particles and their results are minimally affected by the increase of particle image densities up to ppp = 0.0016, and shown reliable results up to ppp = 0.01 (not shown here).

Results for the case '03-astigma1' (used by the teams 'FIL', 'GW', and 'Madeira') and for the case '05-shadow1' (used by the teams 'GW', 'Madeira', and 'MorePath') are shown in Fig. 6a and b, respectively. In general, the teams 'FIL', 'Madeira', and 'MorePath' showed similar errors and recall trends, with small differences. Interestingly, the network used by the team 'Madeira' for the in-plane localization was not trained on a specific flavor, yet it achieved accuracy comparable to methods specifically trained on individual flavors, demonstrating an excellent ability to generalize across different datasets. The use of a conventional cross-correlation approach for depth determination performed very well at low seeding concentrations, but as the seeding was increased, the CNN approach used by 'FIL', 'GW', and 'MorePath' showed significantly improved performance. In particular, the approach used by the team 'GW' shows to be exceptionally robust against overlapping particles, at least up to ppp = 0.0016, maintaining a recall close to 1 and a similar error level. Finally, a separate discussion is required for the case '06-pinhole2', used by the teams 'GW' and 'LaVision', and shown in Fig. 6c. Here, the nature of the images is significantly different, and the use of overall smaller particle images gives an advantage against overlapping particles. In real experiments, this is 'paid' by a lower signal, but, for this Challenge, we used the same average SNR for all cases. Interestingly, the team 'GW' that used the same approach for all flavors, obtained results for the pinhole cases (at least for the low-seeded cases) which were similar to the ones of the other cases, suggesting that the 'pinhole' approach is not intrinsically better than the other flavors. On the other hand, the team 'LaVision' obtained results remarkably accurate on this flavor, with an error of around 0.017 px, 0.013 px, and 0.17 px in the X, Y, and Z direction, respectively. The results were consistent across all particle image densities, maintaining a recall close to 1. This shows that currently, the IPR+STB approach seems to be still superior to machine learning approaches based on CNN. However, the CNN approaches are quickly catching up, with remarkable improvements with respect to earlier applications in the past years [12]. Further improvements are expected in the coming years, especially if the tracking task is included in the processing pipeline. Finally, it should be noted that in this Challenge, an ideal case with no distortion in the image plane was considered, which is not the case for experimental images. Larger uncertainties are therefore expected in experimental images to what reported here.

MFD2

Results for MFD2 were provided by the team 'LaVision' and 'MorePath'. Both teams showed that

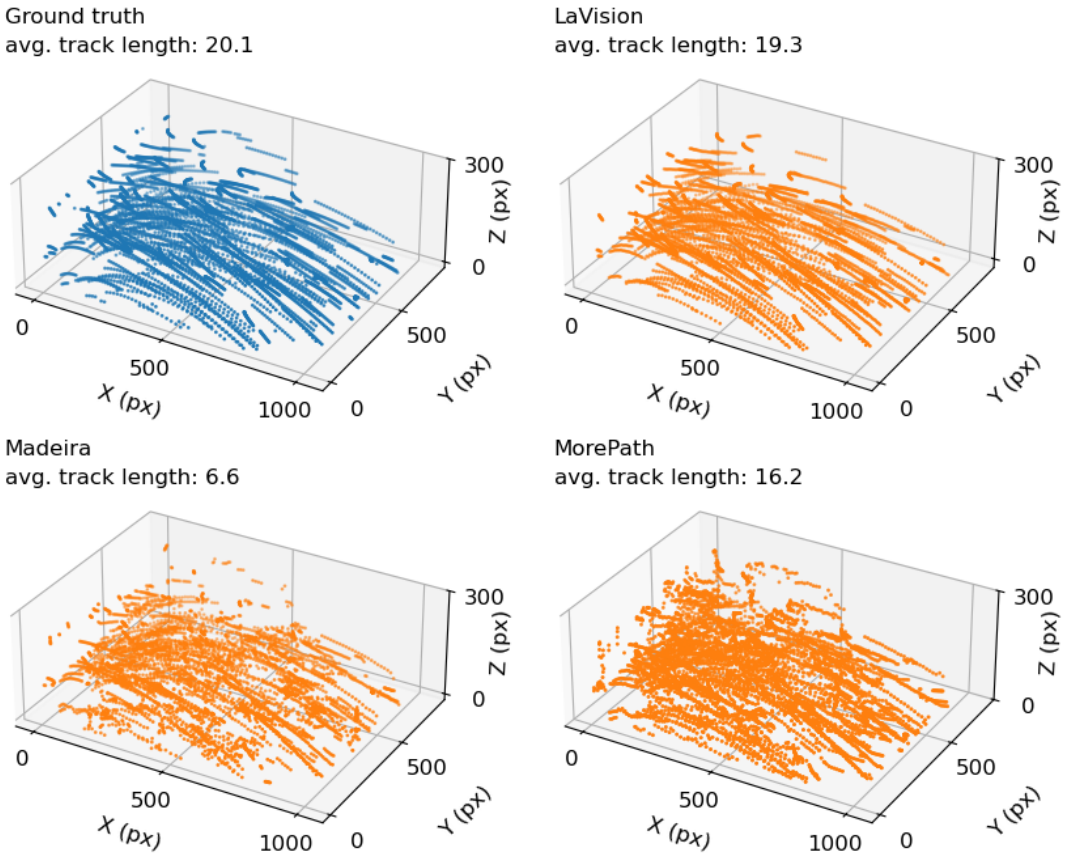


Figure 7. Particle trajectories measured for the MFD3 case.

their code was able to deal with polydispersed particles (30% of the mean value), with a moderate error increase. With respect to the corresponding case with monodispersed particles, 'LaVision' had an error increase with a factor of approximately 2 and 4, in the in-plane and depth position, respectively. 'MorePath' showed a little larger increase with a factor of approximately 5 for in-plane and depth position.

MFD3

Results for MFD3 were provided by the team 'LaVision', 'Madeira', and 'MorePath'. The reconstructed trajectories are presented in Fig. 7. In general, all teams were able to correctly reconstruct the flow field with good accuracy. Also in this case, the team 'LaVision' provided remarkably accurate results, being able to recover most of the tracks, with an average track length of 19.3, only slightly lower than the ground truth value of 20.1 (from a total of 30 consecutive frames).

4. Conclusions

We presented the results of the First Defocus Particle Tracking Challenge. In this conference contribution, the main results are summarized, whereas we postpone a more detailed and quantitative analysis to a follow-up journal publication. From the results submitted by the seven teams in the different experimental and synthetic test cases, several interesting conclusions can be drawn. First of all, the proposed format with ChiB and MFDs proved to be quite successful, and it will be reproposed in future editions of the Challenge. The experimental test cases are suitable for different techniques, and the quality of the results depends not only on the choice of the algorithm, but also on the experience and equipment of the users. All teams provided sensible results using quite different techniques. The synthetic test cases, based on distortion-free images with similar SNR, showed that large progress has been made in DPT methods in the past few years. In particular, methods based on deep learning and CCN are becoming the standard in the field, with four teams out of five among the MFDs' participant. On the other hand, the more accurate results were obtained by a team using a IPR+STB approach, so not based on CCN. It should be noted that this was the only team to incorporate the tracking task into its processing pipeline. Therefore, further improvements in CNN-based techniques can be expected in the future as tracking is integrated into these methods as well.

Acknowledgements

The authors acknowledge financial support by the German Research Foundation (DFG) under the grants No. 537846345. and No. 577000111.

References

[1] C. J. Kähler, T. Astarita, P. P. Vlachos, J. Sakakibara, R. Hain, S. Discetti, R. La Foy, and C. Cierpka. "Main results of the 4th International PIV Challenge". In: *Exp. Fluids* 57 (2016), 1–71. DOI: 10.1007/s00348-016-2173-1.

[2] A. Sciacchitano, B. Leclaire, and A. Schröder. "Main results of the first Lagrangian particle tracking challenge". In: *Proceedings of 14th International Symposium on Particle Image Velocimetry*. 2021.

[3] C. Cierpka and C. J. Kähler. "Particle imaging techniques for volumetric three-component (3D3C) velocity measurements in microfluidics". In: *J. Vis.* 15 (2012), 1–31. DOI: 10.1007/s12650-011-0107-9.

[4] W. Zhou, C. Tropea, B. Chen, Y. Zhang, X. Luo, and X. Cai. "Spray drop measurements using depth from defocus". In: *Meas. Sci. Technol.* 31 (2020), p. 075901. DOI: 10.1088/1361-6501/ab79c6.

[5] J. Klinner and C. E. Willert. "Measurements of the unsteady wall shear stress vector using multi-aperture defocusing microscopic particle tracking velocimetry". In: *Exp. Therm. Fluid Sci.* 163 (2025), p. 111395. DOI: 10.1016/j.expthermflusci.2024.111395.

[6] C. Willert and M. Gharib. "Three-dimensional particle imaging with a single camera". In: *Exp. Fluids* 12 (1992), 353–358. DOI: 10.1007/BF00193880.

[7] C. Cierpka, M. Rossi, R. Segura, and C. Kähler. "On the calibration of astigmatism particle tracking velocimetry for microflows". In: *Meas. Sci. Technol.* 22 (2010), p. 015401. DOI: 10.1088/0957-0233/22/1/015401.

[8] M. Legrand, J. Nogueira, A. Lecuona, and A. Hernando. "Single camera volumetric shadowgraphy system for simultaneous droplet sizing and depth location, including empirical determination of the effective optical aperture". In: *Exp. Therm. Fluid Sci.* 76 (2016), 135–145. DOI: 10.1016/j.expthermflusci.2016.03.018.

[9] R. Azizy, H. Otto, J. König, D. Schreier, C. Weigel, C. Cierpka, and S. Strehle. "A microfluidic magnetohydrodynamic pump based on a thermally bonded composite of glass and dry film photoresist". In: *Micro. Nano. Eng.* 18 (2023), p. 100173. DOI: 10.1016/j.mne.2023.100173.

[10] M. Rossi. "Synthetic image generator for defocusing and astigmatic PIV/PTV". In: *Meas. Sci. Technol.* 31 (2020), p. 017003. DOI: 10.1088/1361-6501/ab42bb.

[11] M. Rossi, S. Sachs, and C. Cierpka. "First Defocus Particle Tracking Challenge: Chip-in-the-Box and multi-flavor datasets". In: *Proceedings of the 16th International Symposium on Particle Image Velocimetry*. 2025.

[12] R. Barnkob, C. Cierpka, M. Chen, S. Sachs, P. Mäder, and M. Rossi. "Defocus particle tracking: a comparison of methods based on model functions, cross-correlation, and neural networks". In: *Meas. Sci. Technol.* 32 (2021), p. 094011. DOI: 10.1088/1361-6501/abfef6.

[13] M. Rossi, A. Marin, and C. Kaehler. "Interfacial flows in sessile evaporating droplets of mineral water". In: *arXiv preprint arXiv:1909.06647* (2019).

[14] B. Park, J. Mauch, H. Kweon, J. Kriegseis, S. Lee, and H. Kim. "STAR-APTV: Deep learning-enabled 3D flow reconstruction in evaporating multicomponent droplets". In: *Measurement* 266 (2026), p. 120368. DOI: 10.1016/j.measurement.2026.120368.

[15] W.-H. Tien. "Development of multi-spectral three-dimensional micro particle tracking velocimetry". In: *Meas. Sci. Tech.* 27 (2016), p. 084010. DOI: 10.1088/0957-0233/27/8/084010.

[16] Z. Yang, T. Cai, S. Lin, and W. Zhou. "3D flow measurement of droplets in a microchannel based on a dual-camera depth from defocus imaging system". In: *Particuology* 112 (2026), 74–86. DOI: 10.1016/j.partic.2026.02.025.

[17] W. Zhou, S. Lin, T. Cai, X. Cai, Z. Yang, and R. Xu. "Rapid full-field scanning imaging for quantification of liquid-borne particulate contaminants". In: *Powder Tech.* 476 (2026), p. 122391. DOI: 10.1016/j.powtec.2026.122391.

[18] M. J. Yamakaitis, A. Rezaiguia, C. Fort, R. Capanna, and P. M. Bardet. "Four-view single-camera plenoptic 3.0 imager for three-dimensional Lagrangian particle tracking in an oscillatory laminar boundary layer". In: *Exp. Fluids* 66 (2025), p. 165. DOI: 10.1007/s00348-025-04095-w.

[19] J. König and C. Cierpka. "Double refractive particle tracking and sizing". In: *Exp. Fluids* 65 (2024), p. 162. DOI: 10.1007/s00348-024-03894-x.

[20] P. Godbersen, D. Schanz, and A. Schröder. "Peak-CNN: improved particle image localization using single-stage CNNs". In: *Experiments in Fluids* 65.10 (2024), p. 153.

[21] A. Speiser, L.-R. Müller, P. Hoess, U. Matti, C. J. Obara, W. R. Legant, A. Kreshuk, J. H. Macke, J. Ries, and S. C. Turaga. "Deep learning enables fast and dense single-molecule localization with high accuracy". In: *Nature methods* 18.9 (2021), pp. 1082–1090.

[22] B. Wieneke. "Iterative reconstruction of volumetric particle distribution". In: *Measurement Science and Technology* 24.2 (2013), p. 024008.

[23] T. Jahn, D. Schanz, and A. Schröder. "Advanced iterative particle reconstruction for Lagrangian particle tracking". In: *Experiments in Fluids* 62.8 (2021), p. 179.

[24] D. Schanz, S. Gesemann, and A. Schröder. "Shake-The-Box: Lagrangian particle tracking at high particle image densities". In: *Experiments in fluids* 57.5 (2016), p. 70.

[25] M. Novara, D. Schanz, N. Reuther, C. J. Kähler, and A. Schröder. "Lagrangian 3D particle tracking in high-speed flows: Shake-The-Box for multi-pulse systems". In: *Experiments in fluids* 57.8 (2016), p. 128.

[26] G. Coutinho, A. S. Moita, A. L. Moreira, and M. Rossi. "DefocusTrackerAI–A Generalized Framework for the Automatic Detection of Defocused Particle Images". In: *arXiv preprint arXiv:2606.00076* (2026).